
Article:
Jin, Saimeng, Tian, Yin, McElroy, Con Robert orcid.org/0000-0003-2315-8153 et al. (3 more authors) (2017) DFT and experimental analysis of aluminium chloride as a Lewis acid proton carrier catalyst for dimethyl carbonate carboxymethylation of alcohols. Catalysis Science and Technology. pp. 4859-4865. ISSN 2044-4761

https://doi.org/10.1039/C7CY01190C

Catalysis Science & Technology

c7cy01190c

We have presented the Graphical Abstract text and image for your article below. This brief summary of your work will appear in the contents pages of the issue in which your article appears.

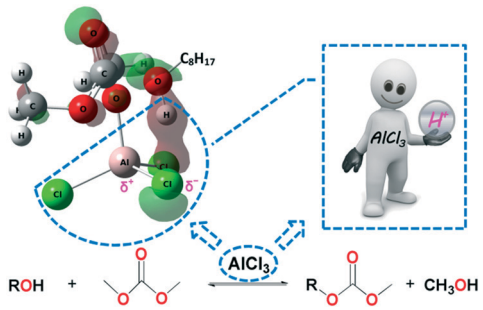

DFT and experimental analysis of aluminium chloride as a Lewis acid proton carrier catalyst for dimethyl carbonate carboxymethylation of alcohols

Saimeng Jin, Yin Tian,* Con Robert McElroy, Dongqi Wang, James H. Clark and Andrew J. Hunt*

In silico and physical experimental data led to a potential acid (AlCl3) catalysed mechanism for DMC carboxymethylation.

Please check this proof carefully. **Our staff will not read it in detail after you have returned it.**

Proof corrections must be returned as a single set of corrections, approved by all co-authors. No further corrections can be made after you have submitted your proof corrections as we will publish your article online as soon as possible after they are received.

Please ensure that:

- The spelling and format of all author names and affiliations are checked carefully. Names will be indexed and cited as shown on the proof, so these must be correct.
- Any funding bodies have been acknowledged appropriately.
- All of the editor's queries are answered.
- Any necessary attachments, such as updated images or ESI files, are provided.

Translation errors between word-processor files and typesetting systems can occur so the whole proof needs to be read. Please pay particular attention to: tables; equations; numerical data; figures and graphics; and references.

Please send your corrections preferably as a copy of the proof PDF with electronic notes attached or alternatively as a list of corrections – do not change the text within the PDF file or send a revised manuscript. Corrections at this stage should be minor and not involve extensive changes.

Please return your **final** corrections, where possible within **48 hours** of receipt, by e-mail to: catalysis@rsc.org. If you require more time, please notify us by email.

Funder information

Providing accurate funding information will enable us to help you comply with your funders' reporting mandates. Clear acknowledgement of funder support is an important consideration in funding evaluation and can increase your chances of securing funding in the future. We work closely with Crossref to make your research discoverable through the Funding Data search tool (http://search.crossref.org/fundref).

Further information on how to acknowledge your funders can be found on our webpage (http://rsc.li/funding-info).

What is Funding Data?

Funding Data (http://www.crossref.org/fundingdata/) provides a reliable way to track the impact of the work that funders support. We collect funding information from our authors and match this information to funders listed in the Open Funder Registry. Once an article has been matched to its funders, it is discoverable through Crossref's search interface.

PubMed Central

Accurate funder information will also help us identify articles that are mandated to be deposited in PubMed Central (PMC) and deposit these on your behalf.

Providing funder information

We have included the funder information you gave us on submission in the table below. The 'Funder name' shown and their associated 'Funder ID' number is written as listed in the Open Funder Registry. **Please check that the funder names and grant numbers in the table are correct.** The funder information should match your acknowledgements. This table will not be included in your final PDF but we will share the data with Crossref so that your article can be found *via* the Funding Data search tool.

Funder name	Funder ID (from the Open Funder Registry)	Award/grant/contract number

If a funding organisation you included on submission of your article is not currently listed in the registry it will not appear in the table above. We can only deposit data if funders are already listed in the Open Funder Registry, but we will pass all funding information on to Crossref so that additional funders can be included in future.

Researcher information

If any authors have ORCID or ResearcherID details that are not listed below, please provide these with your proof corrections.

Please check that the ORCID and ResearcherID details listed below have been assigned to the correct author. Please use this space to add your own unique ORCID iDs and not another researcher's, as errors will delay publication.

Please also update your account on our online manuscript submission system to add your ORCID details, which will then be automatically included in all future submissions. See here for step-by-step instructions and more information on author identifiers.

First (given) name(s)	Last (family) name(s)	ResearcherID	ORCID
Saimeng	Jin		
Yin	Tian		
Con Robert	McElroy		
Dongqi	Wang		
James H.	Clark		0000-0002-5860-2480

Andrew J.	Hunt		0000-0003-3983-8313

Queries for the attention of the authors

Journal: **Catalysis Science & Technology**

Paper: **c7cy01190c**

Title: **DFT and experimental analysis of aluminium chloride as a Lewis acid proton carrier catalyst for dimethyl carbonate carboxymethylation of alcohols**

For your information: You can cite this article before you receive notification of the page numbers by using the following format: (authors), Catal. Sci. Technol., (year), DOI: 10.1039/c7cy01190c.

Editor's queries are marked on your proof like this Q1, Q2, etc. and for your convenience line numbers are indicated like this 5, 10, 15, ...

Please ensure that all queries are answered when returning your proof corrections so that publication of your article is not delayed.

Query Reference	Query	Remarks
Q1	Please carefully check the spelling of all author names. This is important for the correct indexing and future citation of your article. No late corrections can be made.	
Q2	Fig. 4 contains labels (a)–(f), but these do not appear to be mentioned in the caption. Would you like to modify the caption or resupply the artwork (preferably as a TIF file at 600 dots per inch)?	
Q3	Please note that a conflict of interest statement is required for all manuscripts. Please read our policy on Conflicts of interest (http://rsc.li/conflicts) and provide a statement with your proof corrections. If no conflicts exist, please state that "There are no conflicts to declare".	

Catalysis Science & Technology

PAPER

DFT and experimental analysis of aluminium chloride as a Lewis acid proton carrier catalyst for dimethyl carbonate carboxymethylation of alcohols†

Cite this: DOI: 10.1039/c7cy01190c

Saimeng Jin,[a] Yin Tian,*[b] Con Robert McElroy,[a] Dongqi Wang,[c] James H. Clark [a] and Andrew J. Hunt *[ad]

Received 13th June 2017,
Accepted 26th September 2017

DOI: 10.1039/c7cy01190c

rsc.li/catalysis

The Lewis acid catalysed mechanism of dimethyl carbonate (DMC) mediated carboxymethylation of alcohol was investigated experimentally and through computational chemistry methods including density functional theory (DFT). Experimental data showed that catalytic loading of $AlCl_3$ enabled the quantitative carboxymethylation of octanol in less than 20 h, while in the absence of a catalyst only trace product was observed. The geometry of the identified transition states and related energy barriers indicate that the activation energies in $AlCl_3$ catalysed pathways are significantly lower than those in catalyst-free pathways. Theoretical quantum chemistry methods were utilised to explore and analyse the complex of DMC with $AlCl_3$. Natural bond orbital theory analysis and molecular orbital analysis demonstrated that the dipole present in Al–Cl covalent bonding plays a vital role in assisting the proton-transfer process. Most importantly, the reaction mechanism disclosed in this research can aid in the exploration of new Lewis acid catalysed processes in the field of dialkyl carbonate chemistry.

Introduction

Dimethyl carbonate (DMC) is an organic compound of interest due to its various green credentials. It is non-toxic, biodegradable,[1] and considered to be a green solvent.[2] Specifically, DMC is accepted as a safer alternative to traditional highly toxic chemicals such as dimethyl sulphate (DMS) and iodomethane for methylation reactions and phosgene for carboxymethylation reactions.[3] A bimolecular acyl cleavage, nucleophilic substitution ($B_{AC}2$) mechanism has been suggested for base catalysed DMC carboxymethylation, where the carbonyl of DMC undergoes nucleophilic attack, followed by the breaking of the C–O bond to yield the product and methanol.[3,4] Hard-soft acid–base (HSAB) theory[5] was also used to explain the base mediated mechanism of DMC, where a soft nucleophile predominately reacts with the soft methyl group of DMC resulting in methylation, while a hard nucleophile reacts with the hard carbonyl group of DMC to form the carboxymethylation products.[6]

To further explain the reaction mechanisms of dialkyl carbonate chemistry, density functional theory (DFT),[7] a quantum mechanics method for the study of electronic structure of multi-electron systems, has also been successfully employed in a number of studies. DFT gave an insight into the catalytic selectivity of NaY zeolite towards either methylation or carboxymethylation reactions of DMC and the role of the counter ion.[8] DFT, when applied to base catalysed carboxyl methylation reactions of alcohols with various dialkyl carbonates, generated results which were in agreement with experimentally observed trends in leaving and entering groups.[9] When used to examine base catalysed reactions between 1,4-diols and DMC, DFT indicated that cyclisation to form 5 membered ethers was energetically the most favourable reaction product.[10] Although base catalysed reactions of DMC have been extensively covered, no mechanistic studies of Lewis acid or catalyst-free carboxymethylation reactions have been observed in the literature. A recent study reported near quantitative carboxymethylation of primary alcohols in the presence of small quantities of Lewis acid in DMC.[11] Understanding the role of Lewis acids in DMC carboxymethylation reactions and the mechanism by which it occurs, is of

[a] Green Chemistry Centre of Excellence, Department of Chemistry, The University of York, Heslington, York, YO10 5DD, UK
[b] Southwestern Institute of Physics, Chengdu 610041, People's Republic of China. E-mail: tianyin@swip.ac.cn; Tel: +862882850476
[c] Institute of High Energy Physics, Chinese Academy of Sciences, Beijing 100049, People's Republic of China
[d] Materials Chemistry Research Center, Department of Chemistry, Faculty of Science, Khon Kaen University, Khon Kaen, 40002, Thailand. E-mail: andrew@kku.ac.th

† Electronic supplementary information (ESI) available. See DOI: 10.1039/c7cy01190c

significance in expanding the range of catalysts available for green dialkyl carbonate chemistry.

Herein, is reported a combined experimental and DFT study of the mechanism of carboxymethylation of alcohols by DMC with a Lewis acid and in catalyst-free conditions. During this research, $AlCl_3$ and 1-octanol were selected as the representative Lewis acid and aliphatic alcohol, respectively.

Results and discussion

Aluminium chloride catalysed DMC carboxymethylation of 1-octanol

Before *in silico* modelling could be carried out, experimental data for the carboxymethylation of an alcohol by DMC both in the presence of a Lewis acid catalyst and catalyst-free needed to be gathered (Scheme 1). As such, yields of methyl octyl carbonate (MOC) from the reaction of 1-octanol and DMC were obtained every hour over a 19 hours period with and without a catalyst and are shown in Table 1.

The reaction proceeded far more rapidly in the presence of 1% aluminium chloride, giving a near quantitative yield of MOC after 19 hours. Over the same time period, the catalyst-free reaction results in negligible formation of MOC. This indicated that $AlCl_3$ has an excellent ability to efficiently reduce the activation energy towards carboxymethylation of 1-octanol.

Complexation between DMC and $AlCl_3$

DMC contains three electronegative centres each of which could coordinate with $AlCl_3$ through their lone pair of electrons. To confirm this, a combined nuclear magnetic resonance (NMR), Fourier transform infrared spectroscopy (FT-IR) and DFT study were employed to investigate the coordination between DMC and aluminium chloride.

The ^1H NMR and ^{13}C NMR of pure DMC and DMC with $AlCl_3$ (mole ratio of 10 : 1) were acquired (full spectra can be found in ESI† section 1). As is evident in Fig. 1, the ^1H NMR of DMC with aluminium chloride has a higher chemical shift than that of the pure DMC, indicative of deshielding of the CH_3 protons of DMC. Table 2 gives ^{13}C NMR results, again showing deshielding bought about by the presence of $AlCl_3$. This provides evidence that aluminium chloride complexes with DMC.

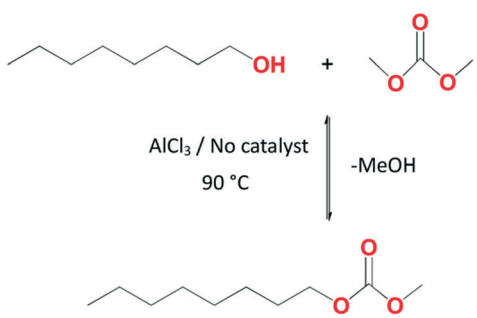

Scheme 1 Synthesis of MOC from 1-octanol and DMC.

The experimental FT-IR spectra of $AlCl_3$, DMC and a mixture of DMC and $AlCl_3$ were also obtained. The strong stretching vibration of Al–O_{ester} (455 cm^{-1}) and Al–$O_{ketonic}$ (488 cm^{-1}) in the mixture of DMC and $AlCl_3$ can be observed, suggesting coordination between $AlCl_3$ and DMC. The theoretical FT-IR spectrum generated by DFT calculation (at the CAM-B3LYP-D3/6-311+G(d,p) level) also supports these results (see ESI† Fig. S8 and S9), where the corresponding two stretching vibration peaks can be found with similar peak interval (32 cm^{-1}) in the range of 390 cm^{-1} to 490 cm^{-1}.

On the basis of NMR and FT-IR results, the formation and the structure of DMC and $AlCl_3$ complexes were investigated by DFT. DFT calculations reveal that the complexation between DMC and $AlCl_3$ results in depolymerisation of dimeric aluminium chloride, as shown in Fig. S10 (see ESI† section 3). Detailed calculations revealed that the complexation between DMC and $AlCl_3$ gives two optimised structures (Fig. 2), where ΔH and ΔG values are negative, suggesting these two complexation processes are both spontaneous and exothermic. As such, both complexes simultaneously exist and can feely interconvert in the system. Further discussion of these calculations can be found in the ESI† (section 3 and 4). Both experimental and *in silico* data demonstrate that aluminium chloride readily complexes with DMC.

Computational study of potential reaction pathways

Calculations carried out on possible transition states for catalyst-free carboxymethylation of 1-ocatnol indicate two favourable pathways (path A and path B) as shown in Scheme 2. Both mechanisms require two molecules of 1-octanol to be present for the reaction to occur. The first alcohol acts as a nucleophile, while the second serves as a bridge to aid in proton transfer. In path A, the nucleophilic 1-octanol molecule (O_{a1}) interacts with the electrophilic carbon atom C_1 and its labile proton H_{a1} transfers to the assisting alcohol O_{a2}. Simultaneously, the proton of the bridging alcohol H_{a2} transfers towards the oxygen atom O_2 (Fig. 4a). The transition state (A-TS) has a six-membered ring structure comprising C_1, O_{a1}, H_{a1}, O_{a2}, H_{a2} and O_2 atoms. The imaginary frequency is 596.2i cm^{-1}, which is mainly associated with the simultaneous creation of C_1–O_{a1}, H_{a1}–O_{a2} and H_{a2}–O_2 bonds, and the destruction of O_{a1}–H_{a1}, O_{a2}–H_{a2} and O_2–C_1 bonds. The imaginary vibrational frequency corresponds to the highest potential energy surface, namely the transition state structure.[12] Path B is a two-step addition/elimination mechanism. As described Scheme 2, this pathway begins with the alcohol assisted addition of R–OH to the C_1=O_1 carbon and proceeds *via* two different transition states (B-TS1 and B-TS2 as shown in Fig. 4). In the first six-membered ring transition state B-TS1, the imaginary frequency is 1247.1i cm^{-1}, associated with the nucleophilic attack of alcohol (O_{a1}) at the C_1 atom, H_{a1} proton transfer from reactant 1-octanol (O_{a1}) towards the assistant 1-octanol (O_{a2}) and subsequent H_{a2} proton transfer from O_{a2} to the carbonyl oxygen O_1. The second step is the elimination process, which

Table 1 The yield of MOC synthesised from 1-octanol and DMC in the presence or absence of $AlCl_3$ at different reaction time[a]

Reaction time (h)	Yield of MOC (%) in the presence of $AlCl_3$[b]	Yield of MOC (%) without catalyst[b]
1	0	0
2	3	0
3	7	0
5	15	0
7	25	<1
9	39	<1
11	49	<1
13	61	<1
15	73	<1
17	88	<1
19	99	<1

[a] Reaction conditions: 1-octanol/DMC/$AlCl_3$ = 6.00 mmol: 240.00 mmol: 0.06 mmol/0.00 mmol; T = 90 °C. [b] Yields were confirmed by GC with tetradecane as internal standard; selectivity >99% towards MOC.

is the breaking of the C_1–O_2 single bond and the simultaneous restoration of the C_1═O_1 carbonyl functionality. As shown in Fig. 3, the DFT calculation indicates that the relative energy of B-TS1 (27.8 kcal mol^{-1}) is lower than that of B-TS2 (31.4 kcal mol^{-1}), which suggests that the latter is the rate-determining step of the pathway. In addition, two single alcohol, 4 membered transition state reaction pathways were calculated, however the activation energy is significantly higher than those of path A and B (see ESI† section 5). This indicates that the formation of the favoured six-membered ring transition state results in reduced ring constraint in proton transfer. As described in Fig. 3, the formation of the different hydrogen bond or coordination bond should lead to the energy differences between the various product complexes (A-PC, B-PC and C-PC). These structures are all shown in ESI† section 8.

The mechanism for $AlCl_3$ catalysed carboxymethylation of 1-octanol with DMC was also determined and involves three different reaction transition states (path C, Scheme 2). In the first step, the imaginary frequency (247.8i cm^{-1}) for the transition state mainly corresponds to nucleophilic attack of 1-octanol (O_{a1}) on the carbonyl (C_1) of DMC and proton transfer of H_{a1} from the alcohol to a chlorine of the Lewis acid. Simultaneously, the creation of the O_2–Al covalent bond occurs. In the second step, the imaginary frequency (392.4i cm^{-1}) for the transition state corresponds to the simultaneous creation of the hydrogen bond H_{a1}–O_3 and the cleaving of the H_{a1}–O_{a1} bond. As shown in Fig. 4e, this $AlCl_3$-assisted proton-transfer step is significant in this pathway, corresponding to the lower energy barriers (14.5 kcal mol^{-1}). The Lewis acid plays the role of proton carrier in this pathway.

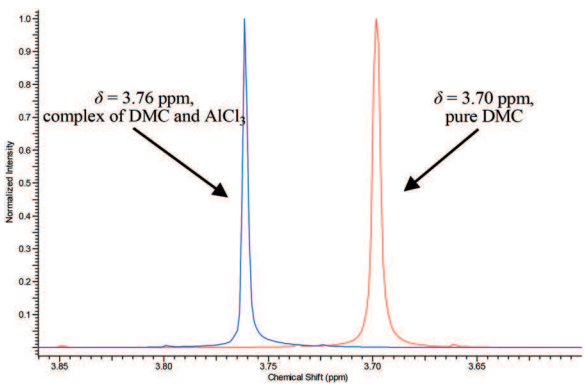

Fig. 1 ^{1}H NMR of pure DMC (red line) and the complex of DMC with $AlCl_3$ (blue line), where the chemical shift of NMR solvent $CDCl_3$ is set as 7.26 ppm in both spectrums.

In addition, natural bond orbital (NBO) theory[13] was performed to analyse Wiberg bond indices (WBIs)[14] and natural atomic charges of these species (Table 3). For species C-IM1, the natural atom charges on aluminium atom and chlorine atom are 1.474 and −0.460, respectively, which relate to the Al–Cl dipole. The WBIs is a measure of the bond order and hence, of the bond strength between two atoms. As depicted in Table 3, the WBIs of H_{a1}–Cl_1 in C-IM1, C-TS2 and C-IM2 are 0.264, 0.825 and 0.284, respectively, suggesting that the δ^+ active proton (H_{a1}) could be stabilised by δ^- chlorine atom (Cl_1) in the proton-transfer process. Furthermore, the WBIs of H_{a1}–O_{a1} in C-IM1 and H_{a1}–O_3 are 0.445 and 0.439, respectively, which also indicated that the active proton H_{a1} transfers from O_{a1} to O_3.

The third step is the inverse of the first step, with proton transfer to O_3 of DMC to form methanol. The above evidence demonstrates that $AlCl_3$ in this reaction plays a vital proton carrier role in assisting hydrogen transfer. As described in Fig. 3, the energy barriers of these three steps are 19.9 kcal mol^{-1}, 14.5 kcal mol^{-1} and 19.2 kcal mol^{-1}, respectively, suggesting that the first step is rate determining. The activation energy required for the rate-determining step of path C (19.9 kcal mol^{-1}) is much lower than those in path A (40.4 kcal mol^{-1}) and path B (31.4 kcal mol^{-1}). Finally, complexation of $AlCl_3$ with the carbonyl oxygen of DMC was studied (ESI† section 6, path D1). This was discounted as a potential mechanism pathway as the activation energy is not only much higher than that of catalysed pathway path C, but also much higher than that of catalyst-free pathway path B, which indicated that structure-B in Fig. 2 is still the active species for carboxymethylation reaction even though structure-A is the high content species.

Table 2 ^{13}C NMR of pure DMC and complex of DMC with $AlCl_3$

	δ (ppm) of methyl carbon of DMC[a]	δ (ppm) of carbonyl carbon of DMC[a]
DMC	54.56	156.18
DMC with $AlCl_3$[b]	54.77	156.31

[a] The chemical shift of NMR solvent $CDCl_3$ was set as 77.00 ppm. [b] Mole ratio of DMC to $AlCl_3$ is 10 : 1.

In this study, geometry optimisations were also carried out using M06-2X/6-311+G(d,p) level of theory. The thermodynamic quantities were calculated at the same level, and the results are described in Table 4 and ESI† section 7. As shown in Table 4, the activation energy barriers obtained by M06-2X and CAM-B3LYP methods, while not identical, are in close enough agreement. This suggests that both computational methods applied in this work are reasonable and reliable.

The theoretical results discussed demonstrate that the Lewis acid $AlCl_3$, can effectively reduce the activation energy for carboxymethylation of 1-octanol by DMC by acting as a vital proton carrier. This proton carrier effect can be clearly illustrated by molecular orbitals analysis. As described in Fig. 5(a), the obvious interaction between the H_{a1} 1s orbital and Cl_1 $3P_z$ orbital can be observed in C-TS1. In C-TS2 (see Fig. 5(b)), the H_{a1} 1s orbital interacts not only with Cl_1 $3P_z$ orbital but also the delocalised π-bonds, which results in a lower energy transition state. Theoretical calculations show good agreement with the experimental results. Experimental activation energy has not been measured since Arrhenius equation, based on collision elementary reaction model, is less suitable for complex organic reactions, and the experimental activation energy obtained by Arrhenius equation may not be comparable to the calculated results.

Conclusions

Until now, reactions between nucleophiles and dimethyl carbonate in the presence of an acid catalyst have neither been widely exploited nor understood. This work utilised a combined experimental and DFT study to gain fundamental understanding of the catalytic effect of aluminium chloride on DMC carboxymethylation reactions. Experimental data showed that catalytic loading of $AlCl_3$ enabled quantitate carboxymethylation of octanol in less than 20 h, while in the absence of a catalyst, only trace amounts of product were observed. *In silico* DFT calculations described possible complexation between DMC and $AlCl_3$ which would increase reactivity towards carboxymethylation.

The geometry of the identified transition states and related energy barriers demonstrated that the activation energy in $AlCl_3$ catalysed reaction pathways are much lower than those in catalyst-free pathways. These results were in good agreement with experimental results. In addition, the natural bond orbital analysis and molecular orbitals analysis demonstrate that, in comparison with the non-catalyst conditions, the dipole present in Al–Cl covalent bonding plays a vital proton carrier role in assisting proton-transfer. These theoretical results are in good agreement with experimental observations.

Most importantly, this research provides a vital basic theory for the exploration and design of new efficient Lewis acid catalysed processes in the field of dialkyl carbonate chemistry. The use of such catalysts will increase the range of substrates available for dialkyl carbonate chemistry (to include acid substrates). The acid catalysed synthetic pathways in combination with the use of *in silico* modelling, applications testing and toxicity measurements may led to the development of greener solvents and products.[19] As demonstrated in this study, acid catalysts offer an efficient method to access carboxymethylation reaction pathways that cannot be investigated utilising traditional base catalysed processes.

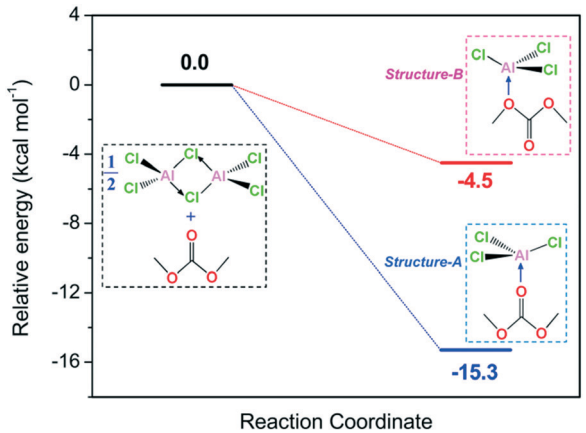

Fig. 2 Relative free energy profiles (ΔG, kcal mol^{-1}) for the complex structure of the different oxygen of DMC interacted with aluminium chloride obtained by the DFT/CAM-B3LYP method.

Experimental section

Materials

1-Octanol 99%, dimethyl carbonate 99%, anhydrous aluminium chloride 99%, methanol 99.9%, acetone 99.9%, chloroform-d ($CDCl_3$, 99.8% D) and tetradecane (analytical standard) were all purchased from Sigma-Aldrich.

Experiment process

To two 100 cm^3 round bottom flasks placed on a multi-point reflux reactor (Radleys, RR98073) were added 6.00 mmol 1-octanol, 240.00 mmol DMC and 50 μL tetradecane (GC internal standard), respectively. To one flask 0.06 mmol anhydrous aluminium chloride was added and then both heated to reflux with agitation. The reactions were run for 19 hours,

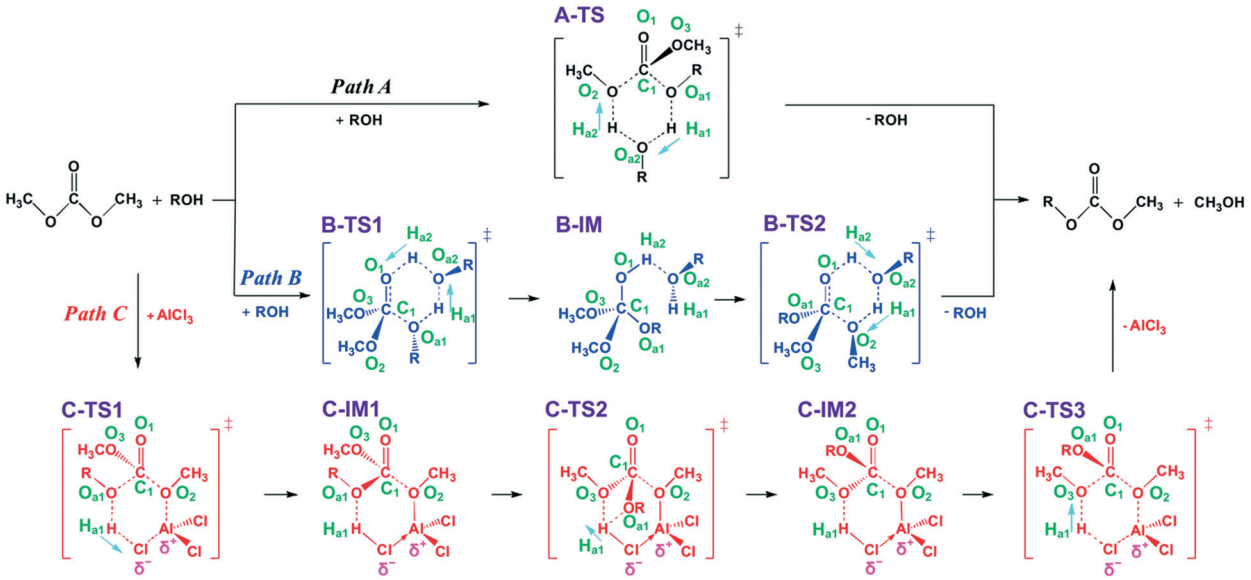

Scheme 2 Reaction pathways of the carboxymethylation of 1-octanol with DMC under the condition of catalyst-free or in the presence of Lewis acid $AlCl_3$ (R = *n*-octyl) obtained by the DFT calculations. The others possible Lewis acid catalysed and non-catalyst reaction pathways are all described in ESI.†

with analysis over time by gas chromatography (GC). Upon completion of the reaction, MOC was separated by distillation under reduced pressure, and its GC, GC-MS, ^{1}H NMR and ^{13}C NMR spectra were obtained. Each reaction was run in triplicate.

MOC: ^{1}H NMR (400 MHz, $CDCl_3$): δ = 0.87 (t, J = 6.40 Hz, 3H, CH_3), 1.19–1.39 (m, 10H, CH_2), 1.65 (m, J = 6.88 Hz, 2H, CH_2), 3.77 (s, 3H, CH_3), 4.12 (t, J = 6.84 Hz, 2H, CH_2) ppm. ^{13}C NMR (400 MHz, $CDCl_3$): δ = 14.05, 22.60, 25.65, 28.63, 29.12, 29.14, 31.73, 54.59, 68.24, 155.87 ppm. GC-MS (relative intensity, 70 eV) *m*/*z*: 117, 112, 103, 97, 84, 77(100), 70, 59, 57, 55, 45, 43, 41.

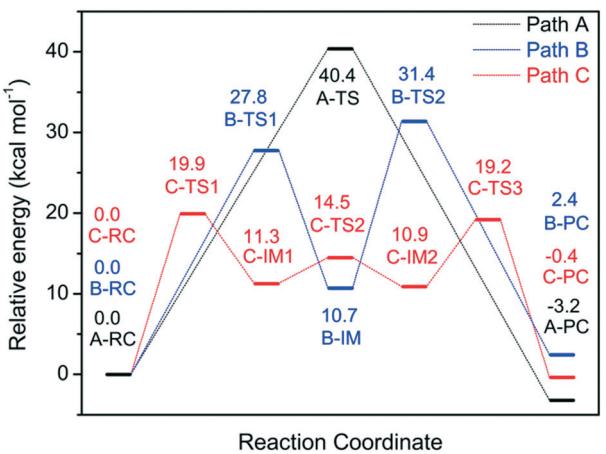

Fig. 3 Relative energy profiles (in kcal mol^{-1}) for the carboxymethylation reaction between DMC and 1-octanol along three pathways obtained by the DFT/CAM-B3LYP method (path A and path B are catalyst-free pathways; path C is $AlCl_3$ catalysed pathway. Relative enthalpy profiles and relative free energy profiles are also described in ESI† Fig. S18 and S19).

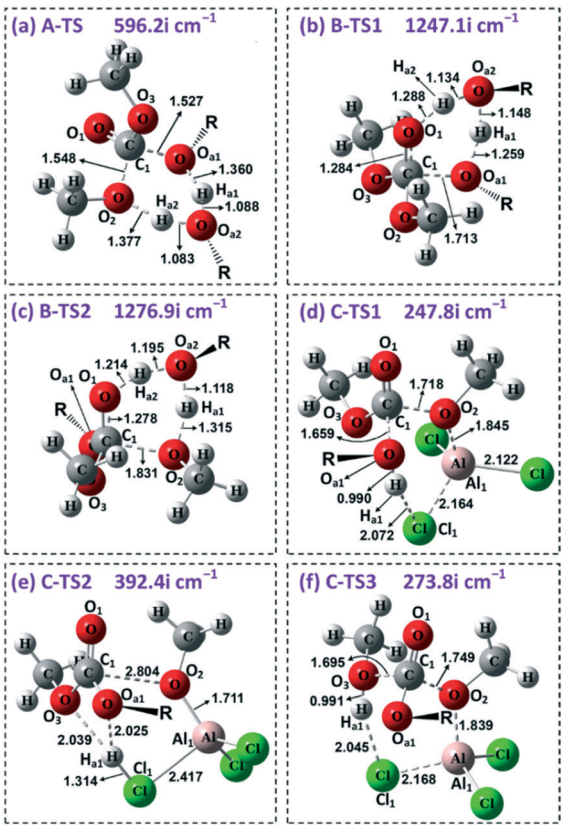

Fig. 4 Optimised transition state (TS) structures along three pathways for the carboxymethylation of 1-octanol with DMC obtained by the DFT/CAM-B3LYP method, and the imaginary frequency of TS and important bond lengths (angstroms) are also shown in this figure (R = *n*-octyl).

Table 3 The natural atom charges (Q) and the Wiberg bond indices (WBIs) between active hydrogen atom (H_{a1}) and carrier chlorine atom (Cl_1) or acceptor oxygen atom (O_{a1} and O_3), obtained by the DFT/CAM-B3LYP method

Species	Q (H_{a1})	Q (Al_1)	Q (Cl_1)	Q (O_{a1})	Q (O_3)	H_{a1}–Cl_1	H_{a1}–O_{a1}	H_{a1}–O_3
C-IM1	0.516	1.474	−0.460	−0.610	−0.529	0.264	0.445	0.003
C-TS2	0.342	1.528	−0.153	−0.589	−0.580	0.825	0.027	0.026
C-IM2	0.508	1.480	−0.454	−0.540	−0.597	0.284	0.003	0.439

GC-FID analysis

During this research, an Agilent 6890 N gas chromatography equipped with a flame ionisation detector (GC-FID) was applied. The GC-FID had a ZB5HT capillary column (30 m × 250 μm × 0.25 μm nominal, max temperature 400 °C) at 20.2 psi constant pressure. The carrier gas utilised in the GC-FID was helium with flow rate at 2.0 cm^3 min^{-1} in constant flow mode. The split ratio used was 10 : 1. The initial oven temperature was held at 50 °C for 4 minutes, after which the temperature was increasing by 10 °C per minute to 300 °C and held at 300 °C for 10 minutes. The temperature of the injector was 300 °C, and the temperature of flame ionisation detector was held at 340 °C. Each of the GC samples consisted of 30 mg product mixture and 1.5 cm^3 acetone as GC solvent.

GC-MS analysis

During the experiment, gas chromatograph-mass spectrometry (GC-MS) was carried out on a Perkin Elmer Clarus 500 GC along with a Clarus 560 S quadrupole mass spectrometer. The instrument had a DB5HT capillary column (30 m × 250 μm × 0.25 μm nominal, max temperature 430 °C). The carrier gas utilised in the GC-MS was helium with flow rate at 1.0 cm^3 min^{-1}. The split ratio was set as 10 : 1. The injector temperature was maintained at 330 °C. The starting temperature of the oven was held at 50 °C for 4 minutes, after which, the temperature was then increased with a rate of 10 °C per minute to 300 °C and held for 10 minutes. The Clarus 500 quadrupole mass spectrum was run in electron ionisation (EI) mode at 70 eV with the source temperature and quadrupole both at 300 °C. The m/z mass scan was in the range of 40 to 640 m/z. The data was collected by PerkinElmer enhanced TurboMass (Ver. 5.4.2) chemical software. The structure of the product was identified by direct comparison of the standard mass spectrum provided in the NIST library (Ver. 2.0). The GC-MS sample consisted of 30 mg product and 1.5 cm^3 acetone as GC solvent.

Table 4 The activation energy barriers (in kcal mol^{-1}) of the catalyst-free pathways and $AlCl_3$ catalysed pathway obtained by M06-2X and CAM-B3LYP methods

Method	Path A	Path B	Path C
M06-2X	39.2	29.0	18.2
CAM-B3LYP	40.4	31.4	19.9

FT-IR analysis

Infrared spectra was recorded on a PerkinElmer Spectrum Two FT-IR spectrophotometer with the PerkinElmer UATR-TWO diamond ATR. PerkinElmer Spectrum software (Ver. 10.03.07.0112) was used to collect and process all the spectral data.

^{1}H NMR and ^{13}C NMR analysis

The ^{1}H NMR and ^{13}C NMR spectrums of the samples in this research were recorded by a JEOL JNM-ECS 400 MHz spectrometer. 100 mg sample was dissolved in 1 cm^3 $CDCl_3$. 16 scans were used for the ^{1}H NMR analysis, and 256 scans were used for ^{13}C NMR analysis. The data of ^{1}H NMR and ^{13}C NMR was analysed by ACD/NMR Processor Academic Edition software (Ver. 12.01).

Quantum chemical calculations

The electronic structure calculations for all of the species have been carried out with Kohn–Sham density functional theory (DFT)[7] methods by using Gaussian 09 program.[15] All of the geometric structures were fully optimised at the CAM-B3LYP[16] level of theory, which included long range correction using the Coulomb-attenuating method. In addition, the M06-2X functional was also applied in this work for comparison. The Grimme's D3-correction with Becke–Johnson damping [D3(BJ)] was used to include London-dispersion correction.[17] The triple split valence basis set 6-311+G(d,p) was used to describe hydrogen, carbon, oxygen, aluminium and chlorine atoms. The default fine grid (75, 302), having 75 radial shells and 302 angular points per shell, was utilised to evaluate the numerical integration accuracy.

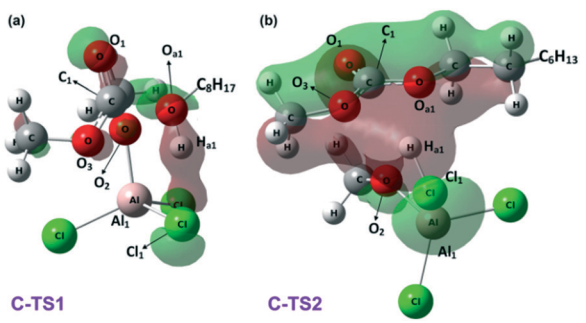

Fig. 5 The important HOMO molecular orbitals of (a) C-TS1 HOMO-25 and (b) C-TS2 HOMO-39 display the interaction between active hydrogen atom H_{a1} and carrier chlorine atom Cl_1. The red and green orbitals represent the plus-minus (±) for the angular part of molecular wave function $Y_{lm}(\theta,\varphi)$.

The harmonic vibrational frequencies were calculated after the geometry optimisations to characterise the nature of the stationary point as a minimum with all positive frequencies or as a transition state with only one imaginary frequency and to provide thermodynamic quantities (at 363.15 °K, 0.1 MPa) such as the enthalpies, entropies and Gibbs free energies. In order to compare the activation energy barriers of different reaction pathways, the energies of reactant complexes (RC) are assumed to be their respective reference values (zero) for different pathways.

In addition, the intrinsic reaction coordinate (IRC)[18] calculations were carried out to verify the transition state (TS) associated with the correct reactant complexes (RC), intermediate (IM) and product complexes (PC). The Wiberg bond indices (WBIs)[14] and natural atomic charges were determined by natural bond orbital (NBO)[13] analysis at the same level.

Conflicts of interest

Q3

Acknowledgements

The authors gratefully acknowledge Dr. John M. Slattery (University of York) and Dr. Duncan J. Macquarrie (University of York) for their helpful suggestions and discussions during this research. Calculations were done on the computational grids in the Supercomputing Centre of Chinese Academy of Sciences (SCCAS).

Notes and references

1 (*a*) M. Bilde, T. E. Møgelberg, J. Sehested, O. J. Nielsen, T. J. Wallington, M. D. Hurley, S. M. Japar, M. Dill, V. L. Orkin, T. J. Buckley, R. E. Huie and M. J. Kurylo, *J. Phys. Chem. A*, 1997, **101**, 3514; (*b*) L. Cassar, *Chim. Ind.*, 1990, **72**, 18.

2 (*a*) B. Schaffner, F. Schaffner, S. P. Verevkin and A. Borne, *Chem. Rev.*, 2010, **110**, 4554; (*b*) F. P. Byrne, S. Jin, G. Paggiola, T. H. M. Petchey, J. H. Clark, T. J. Farmer, A. J. Hunt, C. R. McElroy and J. Sherwood, *Sustainable Chem. Processes*, 2016, **4**, 7.

3 P. Tundo and M. Selva, *Acc. Chem. Res.*, 2002, **35**, 706.

4 P. Tundo, *Pure Appl. Chem.*, 2001, **73**, 1117.

5 (*a*) R. G. Pearson, *J. Am. Chem. Soc.*, 1963, **85**, 3533; (*b*) R. G. Pearson and J. Songstad, *J. Am. Chem. Soc.*, 1967, **89**, 1827.

6 (*a*) P. Tundo, L. Rossi and A. Loris, *J. Org. Chem.*, 2005, **70**, 2219; (*b*) A. E. Rosamilia, F. Aricò and P. Tundo, *J. Org. Chem.*, 2008, **73**, 1559; (*c*) A. E. Rosamilia, F. Aricò and P. Tundo, *J. Phys. Chem. B*, 2008, **112**, 14525.

7 (*a*) P. Hohenberg and W. Kohn, *Phys. Rev.*, 1964, **136**, B864; (*b*) W. Kohn and L. Sham, *Phys. Rev.*, 1965, **140**, A1133.

8 F. Bonino, A. Damin, S. Bordiga, M. Selva, P. Tundo and A. Zecchina, *Angew. Chem., Int. Ed.*, 2005, **44**, 4774.

9 P. Tundo, F. Aricò, A. E. Rosamilia, M. Rigo, A. Maranzana and G. Tonachini, *Pure Appl. Chem.*, 2009, **81**, 1971.

10 F. Aricò, P. Tundo, A. Maranzana and G. Tonachini, *ChemSusChem*, 2012, **5**, 1578.

11 S. Jin, A. J. Hunt, J. H. Clark and C. R. McElroy, *Green Chem.*, 2016, **18**, 5839.

12 J. H. Baraban, P. B. Changala, G. C. Mellau, J. F. Stanton, A. J. Merer and R. W. Field, *Science*, 2015, **350**, 1338.

13 (*a*) J. P. Foster and F. Weinhold, *J. Am. Chem. Soc.*, 1980, **102**, 7211; (*b*) A. E. Reed, R. B. Weinstock and F. Weinhold, *J. Chem. Phys.*, 1985, **83**, 735; (*c*) A. E. Reed, L. A. Curtiss and F. Weinhold, *Chem. Rev.*, 1988, **88**, 899.

14 K. B. Wiberg, *Tetrahedron*, 1968, **24**, 1083.

15 M. J. Frisch, G. W. Trucks, H. B. Schlegel, G. E. Scuseria, M. A. Robb, J. R. Cheeseman, G. Scalmani, V. Barone, B. Mennucci, G. A. Petersson, H. Nakatsuji, M. Caricato, X. Li, H. P. Hratchian, A. F. Izmaylov, J. Bloino, G. Zheng, J. L. Sonnenberg, M. Hada, M. Ehara, K. Toyota, R. Fukuda, J. Hasegawa, M. Ishida, T. Nakajima, Y. Honda, O. Kitao, H. Nakai, T. Vreven, J. A. Montgomery, Jr., J. E. Peralta, F. Ogliaro, M. Bearpark, J. J. Heyd, E. Brothers, K. N. Kudin, V. N. Staroverov, R. Kobayashi, J. Normand, K. Raghavachari, A. Rendell, J. C. Burant, S. S. Iyengar, J. Tomasi, M. Cossi, N. Rega, J. M. Millam, M. Klene, J. E. Knox, J. B. Cross, V. Bakken, C. Adamo, J. Jaramillo, R. Gomperts, R. E. Stratmann, O. Yazyev, A. J. Austin, R. Cammi, C. Pomelli, J. W. Ochterski, R. L. Martin, K. Morokuma, V. G. Zakrzewski, G. A. Voth, P. Salvador, J. J. Dannenberg, S. Dapprich, A. D. Daniels, O. Farkas, J. B. Foresman, J. V. Ortiz, J. Cioslowski and D. J. Fox, *Gaussian 09, revision D.01.*, Gaussian Inc., Wallingford, CT, 2009.

16 T. Yanai, D. Tew and N. Handy, *Chem. Phys. Lett.*, 2004, **393**, 51.

17 (*a*) S. Grimme, J. Antony, S. Ehrlich and H. Krieg, *J. Chem. Phys.*, 2010, **132**, 154104; (*b*) S. Grimme, S. Ehrlich and L. Goerigk, *J. Comput. Chem.*, 2011, **32**, 1456; (*c*) L. Goerigk and J. R. Reimers, *J. Chem. Theory Comput.*, 2013, **9**, 3240.

18 (*a*) K. Fukui, *J. Phys. Chem.*, 1970, **74**, 4161; (*b*) C. Gonzalez and H. B. Schlegel, *J. Chem. Phys.*, 1989, **90**, 2154.

19 S. Jin, F. Byrne, C. R. McElroy, J. Sherwood, J. H. Clark and A. J. Hunt, *Faraday Discuss.*, 2017, **202**, 157–173.